JUNE 1991

WRL Research Report 91/7

Pool Boiling on Small Heat Dissipating Elements in Water at Subatmospheric Pressure

Wade R. McGillis
John S. Fitch
William R. Hamburgen
Van P. Carey

digital **Western Research Laboratory** 250 University Avenue Palo Alto, California 94301 USA

The Western Research Laboratory (WRL) is a computer systems research group that was founded by Digital Equipment Corporation in 1982. Our focus is computer science research relevant to the design and application of high performance scientific computers. We test our ideas by designing, building, and using real systems. The systems we build are research prototypes; they are not intended to become products.

There is a second research laboratory located in Palo Alto, the Systems Research Center (SRC). Other Digital research groups are located in Paris (PRL) and in Cambridge, Massachusetts (CRL).

Our research is directed towards mainstream high-performance computer systems. Our prototypes are intended to foreshadow the future computing environments used by many Digital customers. The long-term goal of WRL is to aid and accelerate the development of high-performance uni- and multi-processors. The research projects within WRL will address various aspects of high-performance computing.

We believe that significant advances in computer systems do not come from any single technological advance. Technologies, both hardware and software, do not all advance at the same pace. System design is the art of composing systems which use each level of technology in an appropriate balance. A major advance in overall system performance will require reexamination of all aspects of the system.

We do work in the design, fabrication and packaging of hardware; language processing and scaling issues in system software design; and the exploration of new applications areas that are opening up with the advent of higher performance systems. Researchers at WRL cooperate closely and move freely among the various levels of system design. This allows us to explore a wide range of tradeoffs to meet system goals.

We publish the results of our work in a variety of journals, conferences, research reports, and technical notes. This document is a research report. Research reports are normally accounts of completed research and may include material from earlier technical notes. We use technical notes for rapid distribution of technical material; usually this represents research in progress.

Research reports and technical notes may be ordered from us. You may mail your order to:

Technical Report Distribution
DEC Western Research Laboratory, WRL-2
250 University Avenue
Palo Alto, California 94301 USA

Reports and notes may also be ordered by electronic mail. Use one of the following addresses:

Digital E-net:	`DECWRL::WRL-TECHREPORTS`
Internet:	`WRL-Techreports@decwrl.dec.com`
UUCP:	`decwrl!wrl-techreports`

To obtain more details on ordering by electronic mail, send a message to one of these addresses with the word ‘‘`help`’’ in the Subject line; you will receive detailed instructions.

Pool Boiling on Small Heat Dissipating Elements in Water at Subatmospheric Pressure

Wade R. McGillis*

John S. Fitch

William R. Hamburgen

Van P. Carey**

June, 1991

---

*Ph.D. candidate at the University of California, Berkeley and a WRL intern.

**Professor of Mechanical Engineering and Applied Science at the University of California, Berkeley.

digital **Western Research Laboratory** 250 University Avenue Palo Alto, California 94301 USA

Abstract

The results of an experimental investigation of pool boiling of water at subatmospheric pressures from small horizontal heat sources are reported. The heat sources are upward-facing copper surfaces submerged in a laterally-confined, finite pool of liquid. The saturated pool boiling heat transfer characteristics and the critical heat flux (CHF) condition were determined in the experiments.

Low pressure boiling of saturated water provides a means of removing heat at high heat flux levels while maintaining low surface temperatures. However, at heat flux levels up to about 60 W/cm^2 the frequency of bubble departure at low pressure is much less than the frequency of bubble departure at higher pressure (atmospheric). With low pressure boiling, only one or two very large bubbles form cyclically on the small heated surface, during the boiling process. This intermittent process may result in large, undesirable temperature oscillations at the heated surface for low pressure boiling. High-frequency surface temperature measurements were obtained in this study which indicate the waiting time between bubbles and the cyclic temperature variation. The waiting time results of this investigation are compared to a simplified heat transfer model and experimental results of previous studies. The nucleate boiling and critical heat flux results indicate that the heater size may have a significant effect on the performance. At low pressures, the few bubbles that form have a departure diameter comparable to the size of the heated surface tested. The apparent effects of heated surface size and pressure on the CHF condition are also discussed.

This is a preprint of a paper that will be presented at the
1991 ASME National Heat Transfer Conference,
Minneapolis, Minnesota, July 28-31, 1991.

Copyright © 1991 ASME

Table of Contents

Nomenclature **vii**
1. Introduction **1**
2. Experimental Apparatus **2**
2.1. The Boiling Process and the Thermosiphon Operation **4**
3. Discussion of Results **8**
3.1. Isolated-Bubble Boiling Regime **8**
3.2. Waiting Time Analysis **8**
3.3. Waiting Time Experimental Results **9**
3.4. Onset of Continuous Boiling - Bubble Growth and Departure Time **10**
3.5. Continuous Boiling Regime - Effect of Pressure **12**
3.6. Critical Heat Flux **14**
4. Conclusions **17**
References **19**

List of Figures

Figure 1: **Schematic diagram of test system and test section used in pool boiling experiments.** **3**

Figure 2: **Photograph of water boiling from a 0.98 cm diameter heated surface at 6 kPa. The average heat flux is 20 W/cm^2.** **5**

Figure 3: **Time response of condenser vapor temperature for different system pressures.** **6**

Figure 4: **Fast Fourier Transform of vapor temperature for a pressure of 6.3 kPa and a surface heat flux of 5 W/cm^2.** **7**

Figure 5: **Comparison between experimental and predicted waiting time versus surface heat flux.** **9**

Figure 6: **Predicted and measured heat flux levels for the transition from intermittent to continuous boiling.** **11**

Figure 7: **Nucleate boiling curves for water on a 1.27 cm square copper heated surface with an emery paper finish. Pressures were maintained at 4, 9, and 101 kPa. Rohsenow correlation plotted for comparison.** **12**

Figure 8: **Effect of heater size on nucleate boiling. The measured CHF condition and the onset to continuous boiling predicted by equation (6) are indicated. Rohsenow correlation plotted for comparison.** **14**

Figure 9: **Effect of heater size and pressure on CHF condition. Data from similar experimental investigations and values predicted by the Zuber model are plotted for comparison.** **15**

Figure 10: **Dimensionless critical heat flux variation with heater characteristic length.** **16**

Nomenclature

A_{heater}	heated element surface area
c_p	liquid specific heat capacity
CHF	critical heat flux
C_{sf}	surface-liquid empirical boiling constant
g	gravity
h_{lv}	specific latent heat of vaporization
k_l	liquid thermal conductivity
L	effective length or diameter of heated surface
OCB	onset of continuous boiling
P	average system pressure
Pr_l	liquid Prandtl number
q''	wall heat flux
q''_m	maximum wall heat flux or critical heat flux
$q''_{m,Z}$	maximum Zuber wall heat flux
r_e	equilibrium bubble radius
R_c	effective surface active cavity size
t_d	bubble growth and departure time
t_w	waiting time
T_s	liquid saturation temperature
T_w	wall or surface temperature

Greek Symbols

α	liquid thermal diffusivity
δ	penetration layer thickness
θ	$T-T_s$, superheat
θ_{ONB}	superheat required for onset of nucleate boiling
θ_w	T_w-T_s, wall superheat
λ_D	most susceptible Taylor unstable wave length
μ_l	liquid viscosity
ρ_l	liquid density
ρ_v	vapor density
σ	liquid surface tension

1. Introduction

In applications where it is desirable to keep the temperature of a boiling surface low, reducing the saturation pressure may be a useful solution. A reduction in the saturation pressure causes a corresponding decrease in the saturation or boiling temperature, allowing a given superheat level to be achieved with a lower surface temperature. This approach is particularly useful when water is used as the boiling liquid. Water is a desirable liquid since it has such a high heat of vaporization, high thermal conductivity, and is non-toxic and non-flamable.

Boiling in sealed vessels is a typical application of low pressure boiling. Heat pipes, thermosiphons, and some heat pump cycles may rely on low pressures to provide low surface temperatures while moving significant quantities of heat. For example, it is often desirable to maintain a low temperature on the heated end of a heat pipe or thermosiphon in spot cooling electronic components. Heat fluxes from current electronic components are approaching 50 W/cm^2. These fluxes are not easily handled by solid heat sinks. Phase-change heat sinks, which operate with a nearly isothermal interior, are becoming increasingly attractive. Low temperature operation of these heat sinks may be prescribed by creating a saturated liquid and vapor state in the vessel at very low pressures. Therefore the boiling occurs in the heated end of the vessel at a low temperature.

The system studied in this investigation consists of boiling of water in a finite pool at subatmospheric and atmospheric pressures from a small horizontal thermosiphon surface. Knowledge of the boiling characteristics of the small heated surface is necessary to insure that steady and safe operating conditions are maintained. In particular, the boiling heat transfer characteristics of low-frequency intermittent bubble departures, the onset to continuous boiling, and the CHF condition. Because intermittent bubble departure may cause undesirable surface temperature oscillations, continuous boiling is desired. The CHF condition prescribes the upper limit on the system operation so as to avoid high surface temperatures characteristic of film boiling.

The characteristics of pool boiling of water at low pressure are known to be much different from the corresponding process at atmospheric pressure. Raben et al. (1965) investigated saturated nucleate pool boiling of water at subatmospheric pressures from a 3.81 cm diameter horizontal heated surface in an extensive pool. Their reported experimental data included the number of active sites on the surface, frequency of bubble departure, and bubble departure diameter for pressures ranging from 1.3 to 101 kPa (101 kPa = 1 atm). The objective of their investigation was to identify the dominant energy transport mechanisms of nucleate boiling and understand how they are affected by pressure. By applying the energy equation to a simple heat transfer model, they presented a theoretical analysis of nucleate boiling. They noted that free convection, vapor-liquid exchange, and the latent heat of vaporization are the possible modes in which energy is transferred during saturated nucleate boiling. For very low pressures, they found that the contribution of latent heat was insignificant compared to the vapor-liquid exchange. Measured heat flux levels ranged from about 8 W/cm^2 at 1.3 kPa to about 19 W/cm^2 at 101 kPa. Heat flux levels were not extended into the regime of vapor slugs and columns or to the critical heat flux limit.

The departure of vapor bubbles in water at low pressure has been the subject of several other studies which have uncovered several important features of this boiling process. Cole and Shul-

man (1967) measured and correlated the affect of pressure on bubble departure diameters from a thin, 1.27 x 10.16 cm horizontal zirconium ribbon.

Van Stralen et al. (1975) studied nucleate boiling in an extensive liquid pool of water at subatmospheric pressures. In their experiments, bubble growth rates, frequencies, and departure diameters for different subatmospheric pressures were investigated.

Recently, the boiling regimes of water and acetone at low pressure in a closed two-phase thermosiphon were examined by Niro and Beretta (1990). Experimental and analytical results of the boiling mechanisms were used to examine the regime between "intermittent" and "fully-developed" boiling. In their experiments, they measured the bubble departure frequencies as a function of pressure and heat flux. They used a circumferentially heated 1.2 and 3.0 cm I.D. diameter by 20 cm vertical tube.

The hydrodynamic CHF model of Zuber (1959), and its extensions to different geometries, (see, for example Lienhard et al. (1973)) seems to provide good predictions of the CHF condition over wide ranges of pressure. It has been demonstrated, however, that the large bubble departure size characteristic of low pressures can lead to intermittent vapor blanketing of small heaters, even at relatively low fluxes. The relationship of this behavior to the postulated hydrodynamic CHF models has not been thoroughly explored.

Van Stralen (1956) reported experimental CHF data for water as a function of pressure from a 0.02 cm heated platinum wire. He found that at low pressure (<10 kPa) the CHF condition occurred over the heated wire immediately at the first appearance of only one vapor bubble. This premature CHF condition did not occur at higher pressures.

Although the boiling characteristics of a discrete, heated element have been well documented at higher pressures, knowledge of how the CHF condition is affected by heater size at subatmospheric pressure is limited. In the present study, the effects of boiling of water from a finite horizontal heat source at subatmospheric and atmospheric pressure are reported. Semi-theoretical models are used as predictive techniques in the determination of the boiling characteristics in a thermosiphon. The critical heat flux characteristics of a finite heated element at subatmospheric and atmospheric pressure are also explored experimentally.

2. Experimental Apparatus

Figure 1 shows the experimental test section and system used in this investigation. The copper test sections were machined to accommodate two cartridge heaters in the bottom end. The top half of the copper piece was milled to provide a long 1.27 x 1.27 cm square or 0.98 cm diameter circular section. Within these sections, 0.8 mm holes were drilled to the center to hold thermocouple wires. The copper and thermocouples were then cast in a low viscosity epoxy.

The size scales that were chosen for this work were comparable to those that might be found in a system used in electronic spot cooling applications. A square boiling surface of 1.6 cm^2 and a round one of 0.75 cm^2 were used since they could accommodate a range of typical electronic component sizes in a thermosiphon application. The main body of the pool boiling container was made with 2.5 cm I.D. tubing.

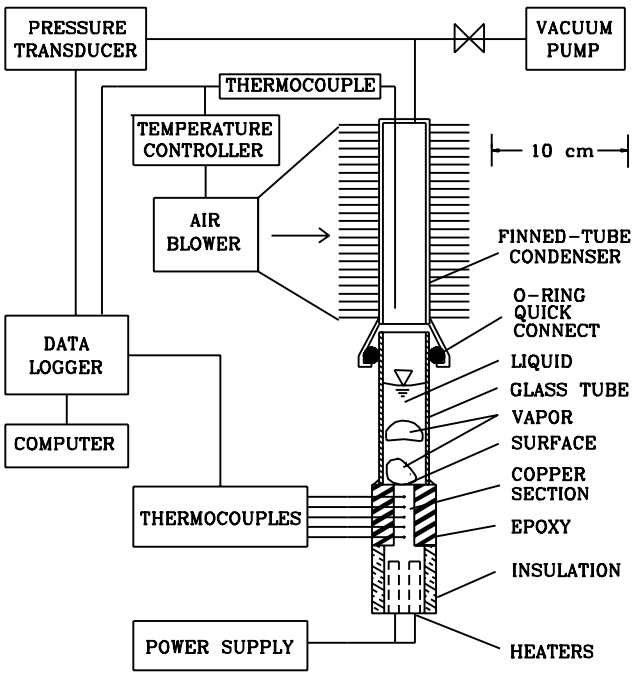

Figure 1: Schematic diagram of test system and test section used in pool boiling experiments.

In order to examine boiling at pressures below 10 kPa for a variety of surface sizes, certain experimental designs were considered. Nucleate boiling is very dependent on cavity size, distribution, and wetting properties. The most difficult extraneous nucleation sites to control were at the interface between the copper test section and the epoxy. This interface had to both maintain a vacuum seal and not become a cavity for nucleation. The Ablebond 342-13 epoxy that was eventually selected, adhered and sealed well enough to the copper so that boiling did not occur at the edge where the copper and epoxy met, even after repeated thermal cycling. Once the epoxy cured, the top surface of the copper could be treated. Excess epoxy was milled down to be flush with the copper surface. The copper/epoxy surface was then finished with #320 emery paper and cleaned with alcohol. The epoxy surface was then bonded to the end of a clear tube to allow observations. The clear tube fit inside an O-ring fitting at the bottom of the condenser so that repeated assembly was simple. The condenser was made of a 12.5 cm long section of copper tubing which had radial copper fins wound and soldered onto its O.D. Heat was removed from the fins with an air blower.

The top end of the condenser tube was equipped with several sensors. A thermocouple probe extended down through the inside of the tube and could be positioned vertically to monitor fluid or vapor temperatures. A transducer measured the internal pressure of the thermosiphon. During initial start up of the system, a valve allowed a two-stage vane-type vacuum pump to pull the internal pressure down to very low values. The liquid was boiled during this step to remove gasses from the internal volume. Any discrepancy between the measured saturation temperature and that predicted from the measured pressure, indicated the presence of non-condensible gasses. Once the gasses were removed, the fluid temperature was maintained by a temperature con-

troller. This controller cycled the blower on and off as needed, and proved able to keep the saturation temperature, T_s, within 1°C during continuous boiling. This maintained the internal pressure constant within 0.27 kPa.

A datalogger recorded the temperatures measured and the system pressure, with a sampling rate of up to 1000 Hz. A linear fit of the measured temperature gradient in the copper section was used to calculate the test section heat flux and the heated surface temperature. In this paper, heat flux is defined as the total heat flow through the end of the test section divided by the wetted area. Experiments and 2-D numerical analyses indicate that the heat losses from the test section were less than 6%, and that the average heat flux at the base of the test surface, q'', could be determined within 3%. Experimental uncertainties in the pressure and differential temperature measurements were 0.1 kPa and 0.1°C, respectively.

Steady state for the entire experiment was determined by monitoring the temperature changes with time via the datalogger and computer. When a particular surface was extended to the critical heat flux condition, the final, highest heat flux for which the system reached steady state for nucleate boiling was used as the CHF data point.

As noted above, experiments in this study were performed with finite, upward-facing heated surfaces of 1.27 x 1.27 cm and 0.98 cm diameter that were submerged in the liquid pool. Data presented in this paper were measured with a stationary liquid pool height of 7.1 cm. However, experiments were performed with different pool heights. For pool heights greater than about 2.5 cm there was no significant variation in the nucleate boiling performance or the CHF condition. The pressures investigated ranged from about 2 to 110 kPa. Heat flux levels were brought to as high as 160 W/cm^2.

2.1. The Boiling Process and the Thermosiphon Operation

The thermosiphon device used in this study could operate in a variety of regimes. When there was no heat supplied to the system, and the liquid and vapor were at thermodynamic equilibrium, the pressure in the system corresponded to the saturation pressure at the system temperature. The liquid became superheated with the application of very low heat fluxes. Heat was removed by evaporation at the liquid-vapor free surface and subsequent condensation occurred at the condenser walls. At higher heat flux levels, the liquid could become superheated enough for bubble growth from cavities on the heated surface. As in any superheated system, the onset of heterogeneous nucleation in a cavity depends on: 1) residual gasses or vapor in the cavity; 2) the size, shape and material of the cavity; 3) the liquid and vapor thermophysical properties; and 4) the amount that the liquid is superheated.

If all of the necessary criteria for bubble growth have been met, a bubble may grow and release from the heated surface. It is expected that when the bubble grows and departs from the surface, colder fluid will replace the highly superheated fluid where the bubble departs. Since bubble growth depends on a sufficient superheating of the liquid in its surrounding, an appreciable amount of time may be required to superheat the liquid in the vicinity of the wall for subsequent bubble growth. This time is termed the "waiting time," t_w. The time it takes the bubble to grow and depart is termed the "bubble departure time," t_d. If, at a particular heat flux and pressure, t_w is greater than t_d, bubble growth off the flat plate is intermittent and the boiling

regime is called "isolated-bubbles." Figure 2 shows a photograph of water boiling in this isolated-bubble regime at a pressure of 6 kPa with an average heat flux of 20 W/cm^2. As can be seen from the photograph, at subatmospheric pressure and at this moderate heat flux level, bubbles grow periodically and from only one or two cavities. At higher heat flux levels, t_w may decrease to be equal to t_d, and the frequency of bubble departure becomes large. The boiling can then considered to be continuous (see Han and Griffith (1965a)).

Figure 2: Photograph of water boiling from a 0.98 cm diameter heated surface at 6 kPa. The average heat flux is 20 W/cm^2.

The waiting time can be determined experimentally for a given surface, fluid, heat flux, and pressure using temperature-time data typical to that shown on Figure 3. Figure 3 shows condenser vapor temperatures versus time measurements for a heat flux level of 5 W/cm^2 for three different system pressures (pressure corresponding to the saturation pressure at the average vapor temperature). Jumps in the condenser vapor temperature indicate boiling activity. Bubbles that are formed on the heated surface eject vapor to the condenser, causing the vapor temperature to suddenly increase. The vapor is then quickly cooled and condensed. The waiting period begins when the vapor's temperature drops exponentially as it is condensed. It continues to cool approaching a limiting temperature. During this time, liquid in the boiler section of the thermosiphon is being heated. The liquid is heated until it becomes superheated enough for the onset of nucleation to occur. The waiting period ends when a bubble is initiated, grows, and departs sending hot vapor to the condenser and cooler liquid to the surface. The cycle is then repeated. This method to determine the waiting times from the temperature characteristics in the vapor region are similar to those used by Niro and Beretta (1990). As indicated in Figure 3, for a constant surface heat flux of 5 W/cm^2, bubble departure frequency increases (waiting time decreases) as the average system pressure is increased. The waiting time was computed with a Fast Fourier Transform computer algorithm applied to the vapor temperature transients. For each pressure and heat flux, the spectrum analysis provided information similar to that shown on Figure 4. The dominant frequency of the Fourier spectra is taken as the inverse of the waiting time.

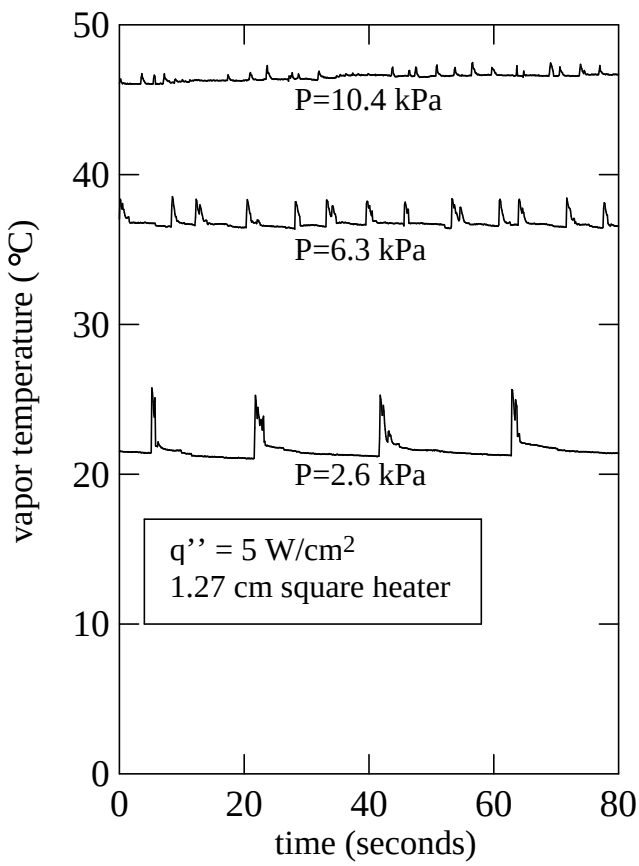

Figure 3: Time response of condenser vapor temperature for different system pressures.

The internal volume of the thermosiphon used in this investigation was not large (116 cm^3), and liquid occupied 30% of it. The finite heater was submerged in the liquid pool. The sudden increase in pressure that occurs during the vapor bubble expansion provides an increase in the saturation temperature. This was the case for low pressure and low heat flux levels. Because the pressure oscillates during this mode of operation, the heat flux versus wall superheat temperature data reported in this paper use averaged values of the the wall temperature and pressure. Continuous bubble growth causes the pressure (and saturation temperature) to remain nearly constant.

The critical heat flux is not a boiling regime but the maximum heat flux attainable before the system makes a transition to film boiling. For many applications, a transition to film boiling is unacceptable because of the very large wall temperature excursions.

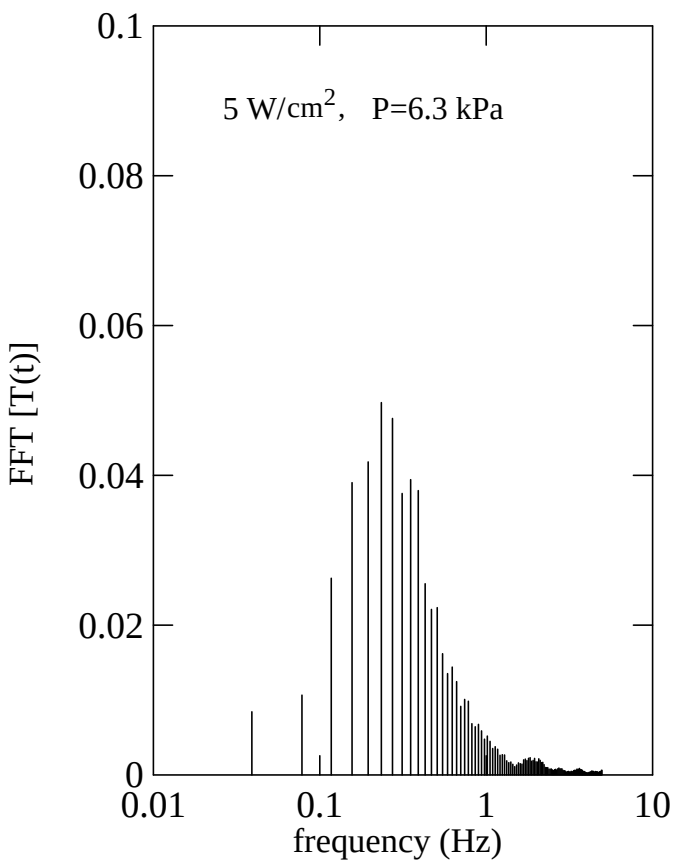

Figure 4: Fast Fourier Transform of vapor temperature for a pressure of 6.3 kPa and a surface heat flux of 5 W/cm^2.

3. Discussion of Results

3.1. Isolated-Bubble Boiling Regime

Understanding the boiling heat transfer characteristics of the isolated bubble regime, the continuous boiling regime, and the CHF condition are necessary to insure that steady and safe operating temperatures of electronics are maintained. In particular, determining the transition from intermittent bubble departure to continuous boiling could be useful in avoiding undesirable surface temperature oscillations. Before the experimental results are presented, an analysis is performed to predict the waiting time. The solution to the analysis of the waiting time is later combined with information about the bubble growth and departure time so as to predict when the transition to continuous boiling occurs.

3.2. Waiting Time Analysis

As discussed above, the criteria for bubble growth depends on surface characteristics, fluid properties, and available superheat. Bubble growth is expected to take place from an active cavity (cavity with residual gasses or vapor) when the surrounding liquid reaches the required superheat (see Hsu (1962), Han and Griffith (1965a), Niro and Beretta (1990)). The following estimate of superheat required for the onset of nucleation, θ_{ONB}, can be derived from the Clausius-Clapeyron equation, $\Delta P \approx \theta \rho_v h_{lv} / T_s$ and the equation of static equilibrium, $\Delta P = 2\sigma / r_e$.

$$\theta_{ONB} = \frac{1.6\,\sigma T_s}{R_c \rho_v h_{lv}} \tag{1}$$

The effective surface cavity size, R_c, is a constant which is presumed to be a function of surface characteristics alone. R_c was postulated by Hsu (1962) to be 0.8 r_e. Equation (1) implies that the superheat required for nucleation is much larger for low pressures since the vapor density is lower. Once a bubble has grown and departed, cooler liquid replaces the fluid adjacent to the wall. A period of time passes when liquid adjacent to the wall is heated as a result of transient conduction. This is called the waiting time, t_w. Han and Griffith argued that since the convection near the solid wall is mitigated due to the no-slip boundary condition at the solid surface, the use of this type of transient penetration layer is a plausible means of determining the temperature distribution of the fluid near the wall.

The solution for the temperature distribution during the transient conduction of heat into a semi-infinite solid (or quasi-static fluid), with the boundary condition of constant heat flux and uniform temperature, is known to be of the form (see Carslaw and Jaeger (1978))

$$\theta(x,t) = \frac{2q''}{k}\left((\alpha t/\pi)^{\frac{1}{2}} e^{\frac{-x^2}{4\alpha t}} - \frac{x}{2} erfc \frac{x}{2\sqrt{\alpha t}} \right) \tag{2}$$

where q'' is the imposed wall heat flux. Using this solution as the basis for estimating t_w, we adopt the frequently used idealization that all of the bubble is to be at or above the required superheat temperature for onset of nucleate boiling. Following Hsu, we enforce this condition by requiring that at $x = R_c$ and $t = t_w$. Executing these steps with a linearized form of equation (2) (valid for short times or small penetration depths), the resulting relation can be solved for t_w, yielding:

$$t_w = \frac{\pi k_l \rho_l c_p}{4 q''^2} \left(\frac{1.6 \sigma T_s}{R_c \rho_v h_{lv}} + \frac{R_c q''}{k} \right)^2 \tag{3}$$

At a given heat flux, the waiting time, t_w, predicted in equation (3) is the time required from the beginning of the thermal layer generation (at bubble departure) to when the bubble temperature reaches the required superheat for bubble growth to begin.

3.3. Waiting Time Experimental Results

The waiting time was measured experimentally for heat flux levels ranging from 2 to 44 W/cm^2 with pressures ranging from 2.02 to 10.4 kPa. The waiting time was experimentally determined for a given surface, fluid, heat flux, and pressure using the condenser vapor temperature versus time data such as that shown on Figure 3. The value of R_c was determined to be 6.38 μm by fitting equation (3) using waiting time data for a 1.27 cm square heat source with a #320 emery paper finish, a heat flux of 5 W/cm^2, and a pressure of 2 kPa. Using this value of R_c and equation (3), t_w versus q'' curves can be generated for different system pressures. As shown in Figure 5, a much longer waiting time for bubble growth to begin is predicted for lower pressures. This is attributed to the greater amount of time required to raise the wall to higher superheat levels.

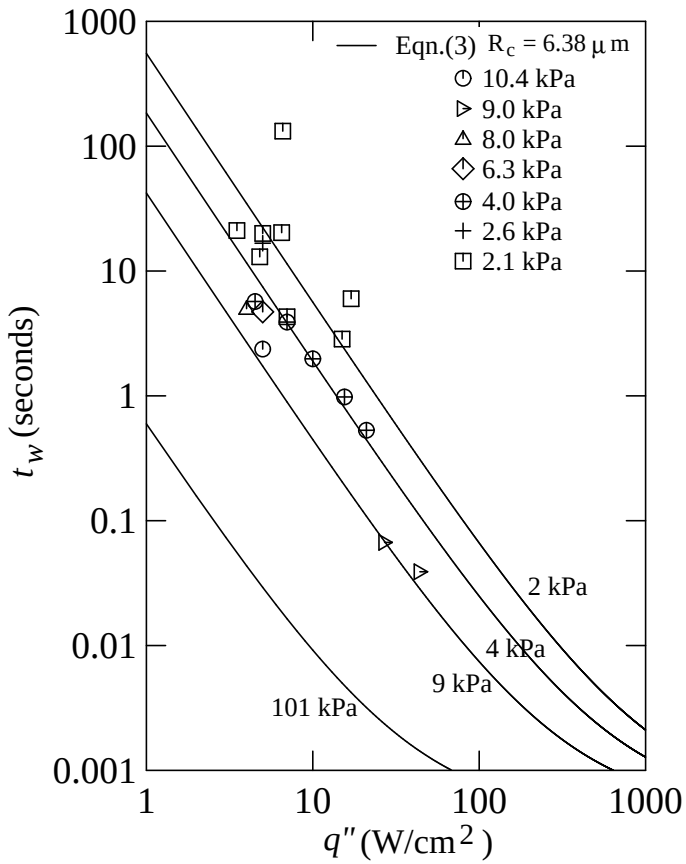

Figure 5: Comparison between experimental and predicted waiting time versus surface heat flux.

In addition to the curves predicted by equation (3), Figure 5 also shows experimentally determined t_w versus q'' data from this study. There appears to be good agreement in the trends between the experimental values and the semi-theoretical predictions of equation (3). Some scatter in the experimental data is expected because it was taken from more than one test specimen. Although each test specimen was prepared in the same manner, there was no assurance that the surface characteristics were identical. Any differences in the surface characteristics results in a different characteristic active cavity size and thus the waiting time could vary.

3.4. Onset of Continuous Boiling - Bubble Growth and Departure Time

The length of time from the beginning of bubble growth to bubble departure depends on how large the bubble must become for release to occur. The time of bubble departure therefore depends on the rate at which the bubble grows to departure size. The departure bubble size is determined from the net effect of forces acting on the bubble as it grows on the surface. Surface tension holds the bubble down. For an upward-facing horizontal surface, buoyancy pulls the bubble up. If the bubble grows rapidly, the inertia associated with the induced liquid flow around the bubble may also tend to pull the bubble away. Bulk liquid motions may also produce lift forces on the bubble causing it to be pulled away. Van Stralen et al. (1975) specifically investigated bubble growth rates in nucleate boiling of water at subatmospheric pressures from a horizontal heat source in an extensive pool. In these experiments, the bubble departure time was measured as a function of pressure. Our approximate fit to their data is provided by the dimensional relation

$$t_d = 0.266\, P^{-0.565} \tag{4}$$

where the bubble departure time, t_d, is in seconds and the pressure, P, is in kPa. Equation (4) proved to be in good quantitative agreement with data.

In general, surface characteristics are not expected to play a significant role in the departure time of a bubble. As noted above, the departure time of a bubble is determined primarily by the bubble growth rate and the forces on the growing bubble. Since the liquid/surface combination used in the study of Van Stralen et al. (1975) is the same as that used in this investigation, the only difference between their system and ours was that their surface was immersed in an extensive liquid pool. In our system the size of the bubbles were comparable to the size of the lateral dimension of the system (the tube width). The finite lateral size of the system would tend to increase the drag on the departing bubble and thus increase the bubble departure time. Since transition to continuous boiling corresponds to t_w=t_d, and equation (4) is expected to slightly underpredict t_d for our thermosiphon system, equations (3) and (4) should provide a reasonable estimate of the threshold condition at which continuous boiling is first achieved. Setting t_w given by equation (3) equal to t_d given by equation (4) and neglecting the term $R_c q''/k$ yields the following relation between the heat flux and pressure at the onset of continuous boiling

$$q''_{OCB} = \frac{1.55\,\sigma T_s P^{0.283}}{R_c \rho_v h_{lv}} \sqrt{\pi k_l \rho_l c_p} \tag{5}$$

The pressure, P, is in kPa. This relationship predicts the heat flux at which the waiting time will be equal to the time it takes for a bubble to grow and depart from the surface. A curve corresponding to equation (5) is plotted on Figure 6. For heat flux levels above the q''_{OCB} predicted by equation (5), boiling is considered to be continuous. Heat flux levels below the predicted q''_{OCB} indicate that t_w is greater than t_d.

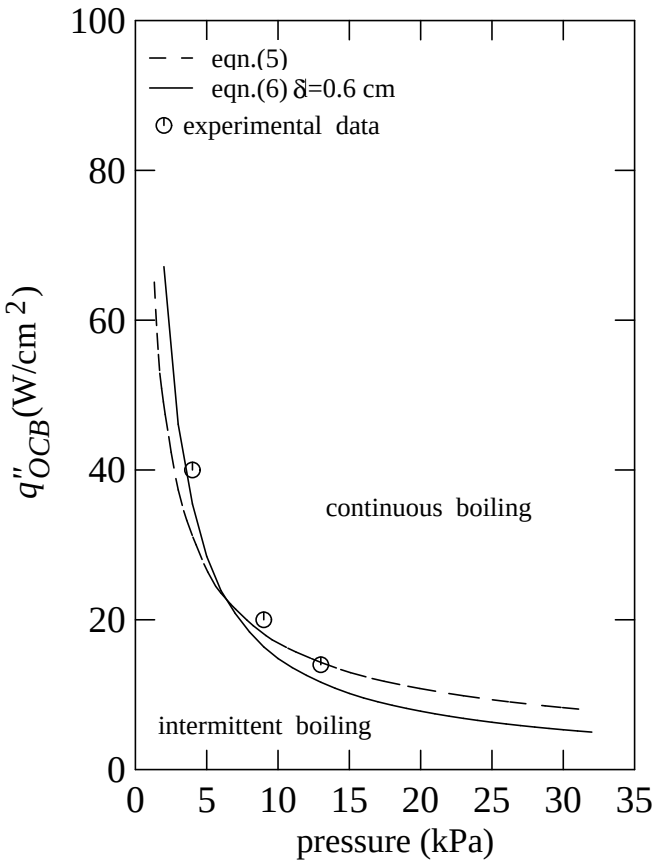

Figure 6: Predicted and measured heat flux levels for the transition from intermittent to continuous boiling.

If the waiting time is greater than the time for bubble growth and release, the boiling is considered intermittent, and significant oscillations in the surface temperature may occur. The magnitude of these oscillations depends on the thermal diffusivity of the solid. For instance, if the waiting time is smaller than the time it takes for a temperature change to penetrate to the thermocouple closest to the surface, the boiling provides nearly constant temperatures at that thermocouple location. The penetration time scale of the solid is $\delta^2/\pi\alpha$, where α is the thermal diffusivity and δ is the transient penetration depth. If this time scale is substituted into equation (3) for the waiting time, using the same approximations to arrive at equation (5), an additional definition for q''_{OCB} is obtained

$$q''_{OCB} = \frac{2.51\,\sigma\,T_s}{\delta\,R_c\,\rho_v\,h_{lv}}\sqrt{k_l\,\rho_l\,c_p\,\alpha_{solid}} \tag{6}$$

where q''_{OCB} is the heat flux where large temperature oscillations in the solid are suppressed at a distance δ from the boiling surface.

Continuous boiling was measured experimentally by determining when temperature oscillations at the closest thermocouple to the surface in the substrate are suppressed to less than 0.2 °C. For several system pressures, continuous boiling heat flux data defined at a thermocouple distance of 0.6 cm from the boiling surface is plotted on Figure 6 for comparison. Equation (6) with δ = 0.6 cm is also plotted in Figure 6 for comparison.

3.5. Continuous Boiling Regime - Effect of Pressure

Figure 7 is a comparison of the nucleate boiling data obtained for the smooth sanded 1.27 by 1.27 cm copper surface in water at three different pressures. A reduction in the pressure for a saturated water system shifted the boiling curve to higher wall superheat (T_w–T_s) levels. However, the decrease in the saturation temperature associated with lower pressures more than compensated for this effect, resulting in lower wall temperatures for a given heat flux. The shift in the boiling curves to higher wall superheats for a given heat flux as pressure decreases may be attributed to a combination of effects. Lower pressures resulted in lower vapor densities and larger bubbles. The lower pressure increased the minimum superheat required for nucleation, resulting in a delayed onset.

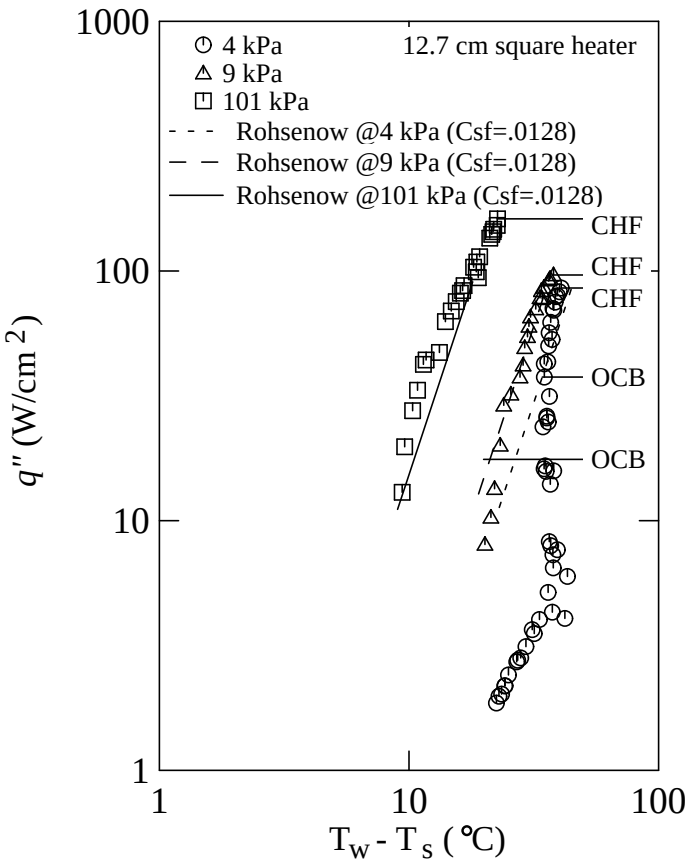

Figure 7: Nucleate boiling curves for water on a 1.27 cm square copper heated surface with an emery paper finish. Pressures were maintained at 4, 9, and 101 kPa. Rohsenow correlation plotted for comparison.

The well-known Rohsenow nucleate-boiling correlation Rohsenow (1952) for water is given by

$$q'' = \mu_l h_{lv} \sqrt{g(\rho_l - \rho_v)/\sigma} \left(\frac{c_p \theta_w}{C_{sf} h_{lv} Pr_l} \right)^3 \tag{7}$$

The value of C_{sf} varies with the liquid/surface combination. For water on copper, the recommended value of C_{sf} varies from 0.0068 (scored copper) to 0.0128 (polished copper). This correlation has been widely tested against water data at pressures above one atmosphere. Its accuracy has not been extensively explored at low pressure, however. Lines corresponding to the Rohsenow correlation of nucleate boiling data for water on a copper surface are also plotted in Figure 7. A value of C_{sf} corresponding to a polished copper surface was used. Although the copper surface was not polished, the fine emery paper finish did provide a somewhat smooth finish. The surface roughness was measured with a surface profilometer to be about 1.3μm rms. Qualitatively, there seems to be a fairly good agreement between our data and this correlation, with properties evaluated at the proper pressures, and the data of this investigation during continuous nucleate boiling, although Rohsenow correlated boiling data for pressures ranging from 101 to 16,936 kPa. Deviations were largest at low pressures and low heat flux levels. At low heat flux levels the boiling is not continuous and the Rohsenow correlation may not apply. The point at which the data intercept the Rohsenow nucleate boiling curve is very near the predictions for the transition to continuous boiling indicated in Figure 7.

The effects of surface finish on nucleate pool boiling of water at subatmospheric pressure in this apparatus were investigated in a separate study. A comparison of boiling curves for copper surfaces with different surface roughness is presented in a companion paper by McGillis et al. (1991). As expected, they showed that a rougher surface increased the heat transfer performance. A larger active cavity generally results in bubble departure at lower wall superheat temperatures. Large surface features, however, do not necessarily mean larger active cavities. Bubble nucleation also depends on nucleate embryos (adsorbed gasses and vapors), vapor density, heat of vaporization, and surface tension. Large cavities have a greater risk of losing their vapor embryos, and consequently may not become active. Since low pressure boiling characteristics are dictated by a small number of large cavities, the boiling heat transfer enhancement with rough surfaces may not be as great as the enhancement at high pressures where there is a significant increase in the number of active sites.

Figure 8 shows a comparison of heat flux versus wall superheat curves for a small round heated surface of diameter 0.98 cm and a 1.27 cm square heated surface, both at 4 kPa. As can be seen, the two surfaces perform similarly. From low heat flux levels where the heat transfer mechanism is primarily natural convection, up through intermittent boiling to the onset of continuous boiling (40 W/cm^2), and through the continuous boiling regime, both surfaces display the same performance. However, although the nucleate boiling behavior is nearly identical, there is a noticeable discrepancy in the critical heat flux condition. At 4 kPa, the CHF condition for the 0.98 cm diameter surface was 25% less than for the 1.27 cm square surface.

3.6. Critical Heat Flux

To avoid the risk of unacceptably high surface temperatures, the ability to predict the CHF condition is useful. The effect of pressure on the critical heat flux condition is illustrated by the maximum heat flux levels shown in Figure 7. For the range of pressures considered, increasing the pressure increased the CHF condition which is consistent with the CHF behavior observed for a variety of other pool boiling circumstances. A commonly used model which predicts the critical heat flux in saturated pool boiling for a surface of infinite extent is Zuber's model mentioned in the introduction. The Zuber critical heat flux is of the form

$$q''_{m,Z} = 0.131\,\rho_v h_{lv}\left(\frac{g(\rho_l-\rho_v)\sigma}{\rho_v^{\,2}}\right)^{\frac{1}{4}} \tag{8}$$

The analysis assumes the critical heat flux is attained when the large vapor jets leaving the surface become Helmholtz unstable. Notice that $q''_{m,Z}$ varies with $\sqrt{\rho_v}$ so that with a given increase in pressure, there is a corresponding increase in the vapor density, and the critical heat flux is increased. An increase in the density of the vapor allows more energy to be removed from the surface for the same volume of vapor departing.

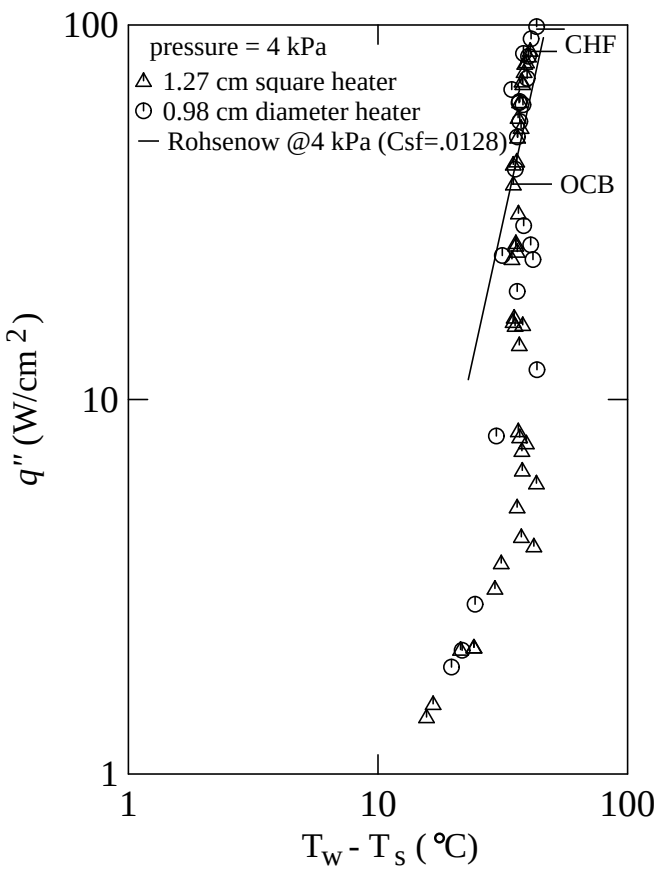

Figure 8: Effect of heater size on nucleate boiling. The measured CHF condition and the onset to continuous boiling predicted by equation (6) are indicated. Rohsenow correlation plotted for comparison.

Figure 9 shows CHF data for distilled water for different heater sizes and pressures. As seen in Figure 9, the critical heat flux data of this investigation are not predicted by the basic Zuber model for a surface of infinite extent (equation (8)) but do approach the Zuber prediction as the pressure is increased. Data from the investigations of Lienhard et al. (1973) and Costello et al. (1965) are also plotted in Figure 9 for comparison. For a pressure of 4 kPa, the 0.98 cm diameter round heater consistently has a somewhat greater critical heat flux than the 1.27 cm square heat source. The CHF data of Costello et al. (1965) for 1.27 and 2.54 cm square heat sources at atmospheric pressure are slightly below that of the present investigation and closely approaches that predicted by the Zuber model. The CHF data of Lienhard et al. (1973) for a round 6.35 cm surface are below that predicted by the Zuber model. Lienhard et al. (1973) argued that since the Zuber's model is for the CHF condition for an infinite surface, it should not predict the case for finite configurations. For finite configurations the characteristic length scale of the finite surfaces becomes extremely important. Lienhard et al. (1973) correlated the critical heat flux mechanisms to be a function of L/λ_D, where λ_D is the Taylor unstable wavelength of the horizontal liquid-vapor interface. For small, isolated heaters of area = A_{heater}, Lienhard et al. (1973) corrected the Zuber critical heat flux as follows:

$$\frac{q''_m}{q''_{m,Z}} = \frac{1.14\,\lambda_D^2}{A_{heater}}, \quad 1 < \frac{L}{\lambda_D} < 2 \tag{9}$$

$$\lambda_D = 2\pi\sqrt{3\sigma / g(\rho_l - \rho_v)} \tag{10}$$

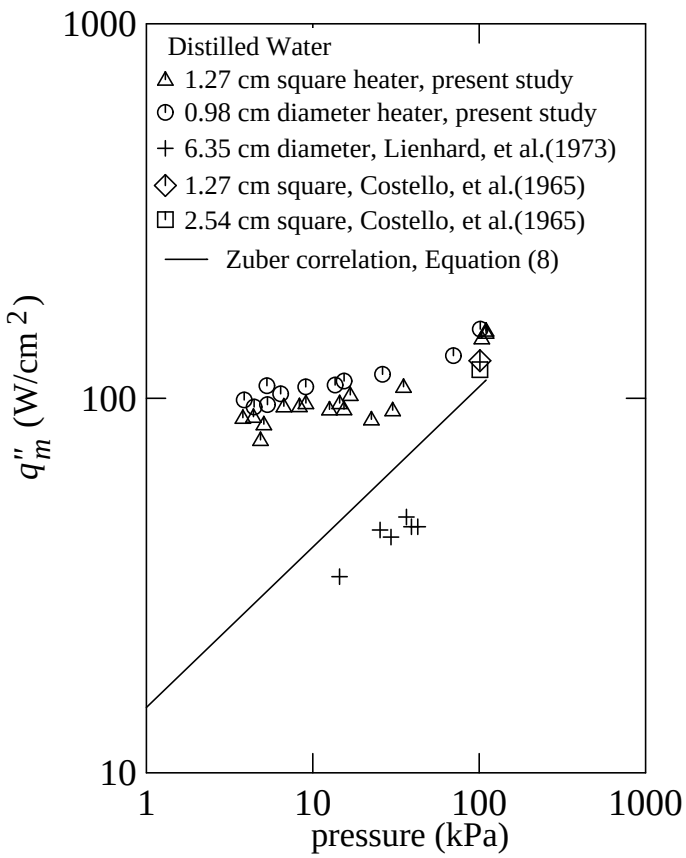

Figure 9: Effect of heater size and pressure on CHF condition. Data from similar experimental investigations and values predicted by the Zuber model are plotted for comparison.

Figure 10 is a plot of the dimensionless heat flux, $q''_m/q''_{m,Z}$, versus the characteristic heater length, L/λ_D. The data from this investigation have a characteristic length, L/λ_D, less than 1, thus falling outside the limited range of applicability of equation (9). For this reason, the hydrodynamic, inviscid model of Zuber (1959) and the corrected model for small geometries by Lienhard et al. (1973) no longer apply; the size of the vapor jet is larger than the heated surface. In Figure 10, the data of Lienhard et al. (1973) lies above the prediction of equation (9), because there were two or more vapor jets leaving the surface. Equation (9) assumed only one vapor jet.

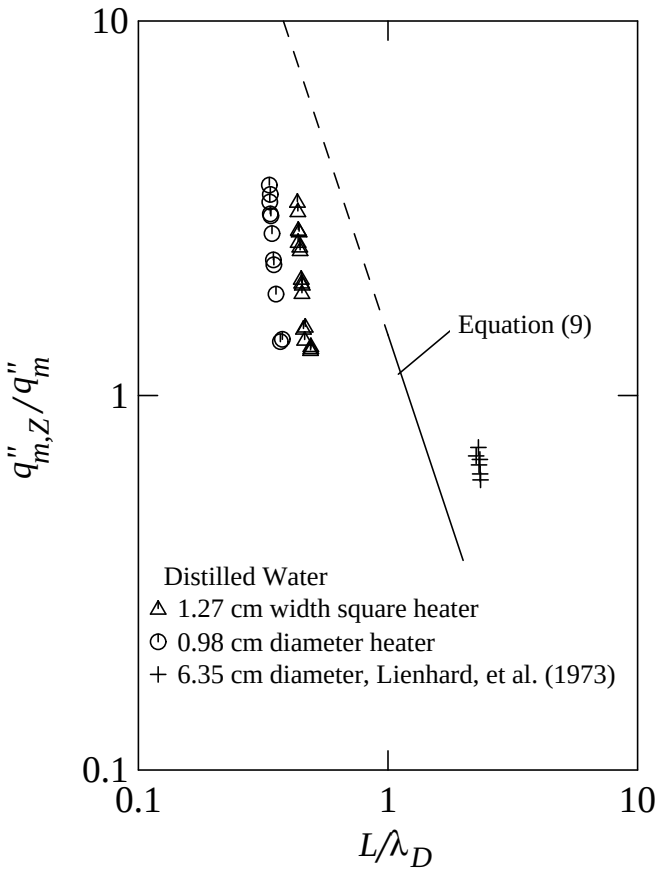

Figure 10: Dimensionless critical heat flux variation with heater characteristic length.

4. Conclusions

The system studied in this investigation consisted of boiling of water in a finite pool at subatmospheric and atmospheric pressures from a small horizontal surface. The boiling characteristics of intermittent bubble departures, the onset to continuous boiling, during continuous boiling, and the CHF condition were investigated. Intermittent bubble departure may cause undesirable surface temperature oscillations, therefore, continuous boiling is desired. The CHF condition prescribes the upper limit on the system operation. Our results support the following conclusions:

1. The regimes of low pressure boiling of water were similar to those previously observed in round tubes, from thin heated wires, and from extensive horizontal surfaces. At low heat flux levels only one or two nucleation sites are active, the frequency of bubble departure is low and the departure diameter is large. The bubble departure frequency increases with heat flux and pressure.

2. Low bubble departure frequencies at low pressure and low heat flux levels cause intermittent downwash of cool liquid adjacent to the wall and subsequent wall temperature fluctuations. For low pressure boiling, a semi-theoretical model was used to predict the waiting time, the time between bubble release and the onset of subsequent bubble growth. Experimental data of this investigation have fairly good agreement with these theoretical predictions.

3. For water at subatmospheric pressures, a correlation was determined for bubble departure time, the time between onset of bubble growth and bubble release. This was combined with the continuous boiling criteria (t_w=t_d) to predict the transition to continuous boiling. For pool boiling of water at very low pressure, heat flux levels as high as 60 W/cm^2 were required to produce a departure frequency high enough to maintain continuous boiling and steady wall temperatures. There was reasonably good agreement between experimental data and this correlation.

4. The commonly used Rohsenow nucleate-boiling correlation agrees well with pressure variation of our continuous boiling data. In the isolated-bubble regime (low heat flux levels and low pressure), however, the data deviates. This is due to the fact that the heat transfer mechanism comprised of conduction into the fluid during intermittent boiling is not as effective as continuous boiling heat transfer, resulting in a reduction in heat transfer performance.

5. For water at subatmospheric pressures, the CHF condition for the small heated surfaces of this study significantly deviates from the infinite surface CHF predictions and the predictions of models which correct for finite size. CHF data of this investigation from small heaters at subatmospheric pressure were as much as 3 times that predicted by the Zuber model. As the pressure is increased toward atmospheric pressure, CHF data of this investigation approach the CHF condition predicted for an infinite flat surface.

References

[1] H. S. Carslaw and J. C. Jaeger.
Conduction of Heat in Solids.
Oxford University Press, Oxford, U. K., 1978.
Second Edition.

[2] R. Cole and H. L. Shulman.
Bubble Departure Diameters at Subatmospheric Pressures.
Chemical Engineering Progresses Symposium Series 62, No. 64:6-16, 1967.

[3] C. P. Costello, C. O. Bock, and C. C. Nichols.
A Study of Induced Convective Effects on Pool Boiling Burnout.
Chemical Engineering Progresses Symposium Series 61:271-280, 1965.

[4] C. Y. Han and P. Griffith.
The Mechanism of Heat Transfer in Nucleate Pool Boiling - Part I: Bubble Initiation, Growth and Departure.
International Journal of Heat and Mass Transfer 8:887-904, 1965.

[5] Y. Y. Hsu.
On the Size Range of Active Nucleation Cavities on a Heating Surface.
ASME Journal of Heat Transfer 84:207-213, 1962.

[6] J. H. Lienhard, V. K. Dhir and D. M. Riherd.
Peak Pool Boiling Heat Flux Measurements on Finite Horizontal Flat Plates.
ASME Journal of Heat Transfer 95:477-482, 1973.

[7] W. R. McGillis, V. P. Carey, J. S. Fitch and W. R. Hamburgen.
Pool Boiling Enhancement Techniques for Water at Low Pressure.
In *Proceedings of the Seventh IEEE Semiconductor Thermal Measurement and Management Symposium*, pages 64-72. 1991 IEEE Semiconductor Thermal Measurement and Management Symposium - SEMI-THERM, Phoenix, Arizona, February, 1991.

[8] A. Niro and G. P. Beretta.
Boiling Regimes in a Closed Two-Phase Thermosyphon.
International Journal of Heat and Mass Transfer 33(10):2099-2110, 1990.

[9] I. A. Raben, R. T. Beaubouef, and G. E. Commerford.
A Study of Heat Tranfer in Nucleate Pool Boiling of Water at Low Pressure.
Chemical Engineering Progresses Symposium Series 61(57):249-257, 1965.

[10] W. M. Rohsenow.
Handbook of Heat Transfer - A Study of Heat Transfer in Nucleate Pool Boiling of Water at Low Pressure.
McGraw-Hill, New York, 1952.
W. M. Rohsenow and J. P. Hartnett ed., Section 13.

[11] S. J. D. Van Stralen.
Heat Transfer to Boiling Binary Liquid Mixtures at Atmospheric and Subatmospheric Pressures.
Chemical Engineering Sciences 5:290-296, 1956.

[12] S. J. D. Van Stralen, R. Cole, W.M. Sluyter, and M. S. Sohal.
Bubble Growth Rates in Nucleate Boiling of Water at Subatmospheric Pressures.
International Journal of Heat and Mass Transfer 18:655-669, 1975.

[13] N. Zuber.
Hydrodynamic Aspects of Boiling Heat Transfer.
AEC Report No. AECU-4439, Physics and Mathematics, AEC, , 1959.

WRL Research Reports

‘‘Titan System Manual.’’
Michael J. K. Nielsen.
WRL Research Report 86/1, September 1986.

‘‘Global Register Allocation at Link Time.’’
David W. Wall.
WRL Research Report 86/3, October 1986.

‘‘Optimal Finned Heat Sinks.’’
William R. Hamburgen.
WRL Research Report 86/4, October 1986.

‘‘The Mahler Experience: Using an Intermediate Language as the Machine Description.’’
David W. Wall and Michael L. Powell.
WRL Research Report 87/1, August 1987.

‘‘The Packet Filter: An Efficient Mechanism for User-level Network Code.’’
Jeffrey C. Mogul, Richard F. Rashid, Michael J. Accetta.
WRL Research Report 87/2, November 1987.

‘‘Fragmentation Considered Harmful.’’
Christopher A. Kent, Jeffrey C. Mogul.
WRL Research Report 87/3, December 1987.

‘‘Cache Coherence in Distributed Systems.’’
Christopher A. Kent.
WRL Research Report 87/4, December 1987.

‘‘Register Windows vs. Register Allocation.’’
David W. Wall.
WRL Research Report 87/5, December 1987.

‘‘Editing Graphical Objects Using Procedural Representations.’’
Paul J. Asente.
WRL Research Report 87/6, November 1987.

‘‘The USENET Cookbook: an Experiment in Electronic Publication.’’
Brian K. Reid.
WRL Research Report 87/7, December 1987.

‘‘MultiTitan: Four Architecture Papers.’’
Norman P. Jouppi, Jeremy Dion, David Boggs, Michael J. K. Nielsen.
WRL Research Report 87/8, April 1988.

‘‘Fast Printed Circuit Board Routing.’’
Jeremy Dion.
WRL Research Report 88/1, March 1988.

‘‘Compacting Garbage Collection with Ambiguous Roots.’’
Joel F. Bartlett.
WRL Research Report 88/2, February 1988.

‘‘The Experimental Literature of The Internet: An Annotated Bibliography.’’
Jeffrey C. Mogul.
WRL Research Report 88/3, August 1988.

‘‘Measured Capacity of an Ethernet: Myths and Reality.’’
David R. Boggs, Jeffrey C. Mogul, Christopher A. Kent.
WRL Research Report 88/4, September 1988.

‘‘Visa Protocols for Controlling Inter-Organizational Datagram Flow: Extended Description.’’
Deborah Estrin, Jeffrey C. Mogul, Gene Tsudik, Kamaljit Anand.
WRL Research Report 88/5, December 1988.

‘‘SCHEME->C A Portable Scheme-to-C Compiler.’’
Joel F. Bartlett.
WRL Research Report 89/1, January 1989.

‘‘Optimal Group Distribution in Carry-Skip Adders.’’
Silvio Turrini.
WRL Research Report 89/2, February 1989.

‘‘Precise Robotic Paste Dot Dispensing.’’
William R. Hamburgen.
WRL Research Report 89/3, February 1989.

''Simple and Flexible Datagram Access Controls for Unix-based Gateways.''
Jeffrey C. Mogul.
WRL Research Report 89/4, March 1989.

''Spritely NFS: Implementation and Performance of Cache-Consistency Protocols.''
V. Srinivasan and Jeffrey C. Mogul.
WRL Research Report 89/5, May 1989.

''Available Instruction-Level Parallelism for Superscalar and Superpipelined Machines.''
Norman P. Jouppi and David W. Wall.
WRL Research Report 89/7, July 1989.

''A Unified Vector/Scalar Floating-Point Architecture.''
Norman P. Jouppi, Jonathan Bertoni, and David W. Wall.
WRL Research Report 89/8, July 1989.

''Architectural and Organizational Tradeoffs in the Design of the MultiTitan CPU.''
Norman P. Jouppi.
WRL Research Report 89/9, July 1989.

''Integration and Packaging Plateaus of Processor Performance.''
Norman P. Jouppi.
WRL Research Report 89/10, July 1989.

''A 20-MIPS Sustained 32-bit CMOS Microprocessor with High Ratio of Sustained to Peak Performance.''
Norman P. Jouppi and Jeffrey Y. F. Tang.
WRL Research Report 89/11, July 1989.

''The Distribution of Instruction-Level and Machine Parallelism and Its Effect on Performance.''
Norman P. Jouppi.
WRL Research Report 89/13, July 1989.

''Long Address Traces from RISC Machines: Generation and Analysis.''
Anita Borg, R.E.Kessler, Georgia Lazana, and David W. Wall.
WRL Research Report 89/14, September 1989.

''Link-Time Code Modification.''
David W. Wall.
WRL Research Report 89/17, September 1989.

''Noise Issues in the ECL Circuit Family.''
Jeffrey Y.F. Tang and J. Leon Yang.
WRL Research Report 90/1, January 1990.

''Efficient Generation of Test Patterns Using Boolean Satisfiablilty.''
Tracy Larrabee.
WRL Research Report 90/2, February 1990.

''Two Papers on Test Pattern Generation.''
Tracy Larrabee.
WRL Research Report 90/3, March 1990.

''Virtual Memory vs. The File System.''
Michael N. Nelson.
WRL Research Report 90/4, March 1990.

''Efficient Use of Workstations for Passive Monitoring of Local Area Networks.''
Jeffrey C. Mogul.
WRL Research Report 90/5, July 1990.

''A One-Dimensional Thermal Model for the VAX 9000 Multi Chip Units.''
John S. Fitch.
WRL Research Report 90/6, July 1990.

''1990 DECWRL/Livermore Magic Release.''
Robert N. Mayo, Michael H. Arnold, Walter S. Scott, Don Stark, Gordon T. Hamachi.
WRL Research Report 90/7, September 1990.

''Pool Boiling Enhancement Techniques for Water at Low Pressure.''
Wade R. McGillis, John S. Fitch, William R. Hamburgen, Van P. Carey.
WRL Research Report 90/9, December 1990.

''Writing Fast X Servers for Dumb Color Frame Buffers.''
Joel McCormack.
WRL Research Report 91/1, February 1991.

‘‘Analysis of Power Supply Networks in VLSI Circuits.’’
Don Stark.
WRL Research Report 91/3, April 1991.

‘‘Procedure Merging with Instruction Caches.’’
Scott McFarling.
WRL Research Report 91/5, March 1991.

‘‘Don’t Fidget with Widgets, Draw!.’’
Joel Bartlett.
WRL Research Report 91/6, May 1991.

‘‘Pool Boiling on Small Heat Dissipating Elements in Water at Subatmospheric Pressure.’’
Wade R. McGillis, John S. Fitch, William R. Hamburgen, Van P. Carey.
WRL Research Report 91/7, June 1991.

WRL Technical Notes

‘‘TCP/IP PrintServer: Print Server Protocol.’’
Brian K. Reid and Christopher A. Kent.
WRL Technical Note TN-4, September 1988.

‘‘TCP/IP PrintServer: Server Architecture and Implementation.’’
Christopher A. Kent.
WRL Technical Note TN-7, November 1988.

‘‘Smart Code, Stupid Memory: A Fast X Server for a Dumb Color Frame Buffer.’’
Joel McCormack.
WRL Technical Note TN-9, September 1989.

‘‘Why Aren’t Operating Systems Getting Faster As Fast As Hardware?’’
John Ousterhout.
WRL Technical Note TN-11, October 1989.

‘‘Mostly-Copying Garbage Collection Picks Up Generations and C++.’’
Joel F. Bartlett.
WRL Technical Note TN-12, October 1989.

‘‘Limits of Instruction-Level Parallelism.’’
David W. Wall.
WRL Technical Note TN-15, December 1990.

‘‘The Effect of Context Switches on Cache Performance.’’
Jeffrey C. Mogul and Anita Borg.
WRL Technical Note TN-16, December 1990.

‘‘MTOOL: A Method For Detecting Memory Bottlenecks.’’
Aaron Goldberg and John Hennessy.
WRL Technical Note TN-17, December 1990.

‘‘Predicting Program Behavior Using Real or Estimated Profiles.’’
David W. Wall.
WRL Technical Note TN-18, December 1990.

‘‘Systems for Late Code Modification.’’
David W. Wall.
WRL Technical Note TN-19, June 1991.